Arabian Journal of Chemical and Environmental Research

Vol. 09 Issue 2 (2022) 232–243

Design of heat exchanger for the production of magnesium oxide nanofluid using sol-gel method

Anisa Noorlela[1], Asep Bayu Dani Nandiyanto[2*], Risti Ragadhita[3] and Teguh Kurniawan[4]

[1,2,3]*Departemen of Chemistry, Universitas Pendidikan Indonesia, Bandung, Indonesia*
[4]*Departemen of Chemical Engineering, Universitas Ageng Tirtayasa, Serang, Indonesia*

Received 25 November 2022, Revised 25 Dec 2022, Accepted 27 Dec 2022

***Cited as** : A. Noorlela, A. B. D. Nandiyanto, R. Ragadhita and T. Kurniawan, Design of heat exchanger for the production of magnesium oxide nanofluid using Sol-Gel method, Arab. J. Chem. Environ. Res. 09(2) (2022) 232-243*

Abstract

This study aims to analyze and development a heat exchanger (HE) design in a magnesium oxide (MgO) production process using the sol-gel method. The HE equipment used has a shell length specification of 0.228 mm; shell diameter 0.203 mm; outer tube diameter 0.0254 m; inner tube diameter 0.0211 mm; wall thickness 0.0021 mm; tube length 5.4864; and tube pitch 0.02778. The method used in this study uses the Microsoft Excel application to perform calculations manually. The results showed that the HE design on the one-pass type shell and tube was laminar flow, with an effectiveness value of 93.70%. Thus, the HE with one-pass shell and tube meets the standard requirements based on the effectiveness value. However, when viewed from a factor perspective, the fouling value has not been calculated. The results of this study are expected to be used as learning media for the design process, operating mechanisms, and HE performance analysis.

Keywords: Magnesium oxide nanoparticles, shell and tube, heat exchanger, effectiveness, education

*Corresponding author.
E-mail address: nandiyanto@upi.edu

1. Introduction

Heat exchanger (HE) is a tool that can be used to transfer heat from one fluid to another with high to low temperature changes using a separator medium so that the heat transfer process occurs optimally [1-4]. In industrial-scale process activities, this tool is very important because it is widely applied in

industrial plants such as oil refineries, petrochemicals, natural gas industries, refrigeration, and power plants [3,5]. HE has several advantages, including being able to save costs because the costs incurred are low and produce good performance characterized by high thermal efficiency [6]. HE consists of several thin plates joined by a parallel-plate framework [7]. HE design development is still needed to improve system performance and efficiency in accordance with the overall work function of the tool [8]. One of the most popular HE is the shell and tube heat exchanger [9]. Several types of heat exchangers are usually used to heat products or cool products. Therefore, in order to develop technology, especially heat exchanger equipment, it is necessary to carry out technical design of the tool or technological engineering to obtain better results.

Magnesium oxide (MgO) is an important functional metal oxide that has been widely used in various fields. MgO can be used for ceramic materials because it has a high melting point that makes it fire resistant, has a strong surface, is water resistant, soundproof, resistant to attack by mold, mildew and decay. MgO has excellent optical, electrical, thermodynamic, electronic and mechanical properties. In the industrial world, MgO is usually used to make materials that function as heat-resistant walls in furnaces, electrical insulators, food packaging, cosmetics, pharmaceutical manufacturing [10], catalysts [11], bactericidal properties [12], photocatalytic [13], adsorbents [14], optical properties [15], electrochemical biosensors [16], refractory materials, paints, and superconductors [17].

Magnesium oxide nanoparticles are metal oxide nanoparticles which are highly ionic in nature with a very high surface area and an unusual crystal morphology [17]. Magnesium oxide nanoparticles have been widely used because they have unique properties, namely a wide bandgap, the ability to maintain thermodynamic stability, a low dielectric constant, and a low index of refraction [18]. Several methods can be used in the synthesis of magnesium oxide nanoparticles, including combustion [19], synthesis of plant extracts [20], sonochemical synthesis [21], solid-state synthesis [22], and sol-gel synthesis [23]. In this research, synthesis of magnesium oxide by sol-gel method was used. The sol-gel method is a widely used method for synthesizing magnesium oxide nanoparticles because the process is simple, the product yield is quite high, and the reaction temperature is low. In addition, the sol-gel method is relatively inexpensive to obtain magnesium oxide nanoparticles with a narrow size distribution and larger surface area which is very important to overcome the problem of low reactivity and catalytic ability [24].

Several studies on the design of heat exchangers have been carried out [25-27]. For the referred studies, we analyze and evaluate the experimental process. Therefore, the aim of this research is to design and develop HE applications for the production of MgO nanoparticles from arabic gum as a base material. Various literatures on the synthesis of MgO have been studied [28-30]. The designed heat exchanger is a shell and tube type which is designed simply by referring to the existing design rules. This study is

expected to be a useful reference in designing and developing heat exchangers, as well as a learning method starting from process design, working mechanism, to HE performance.

2. Materials and methods

2.1. Production of Magnesium Oxide Nanoparticles

The special processing conditions and preparation procedures for producing magnesium oxide (MgO) nanoparticles are shown in Figure 1. The synthesis procedure for MgO nanoparticles was taken from experiments by Sutapa et al. (2018) using $Mg(CH_3COO)_2.4H_2O$ and $C_2O_4.2H_2O$ raw materials [31]. Furthermore, as much as 50 grams of the raw material was dissolved in 150 mL of methanol with constant heating using a magnetic stirrer. The constant heating process will produce a clear colored mixture. The mixture obtained was adjusted to pH 5 by adding oxalic acid drop by drop into the solution and followed by a stirring process until a white gel was obtained. The resulting gel was cooled to room temperature and left for 12 hours so that the gelation process was complete. The gel was then filtered using Whatman-42 filter paper to separate the gel and the solution.

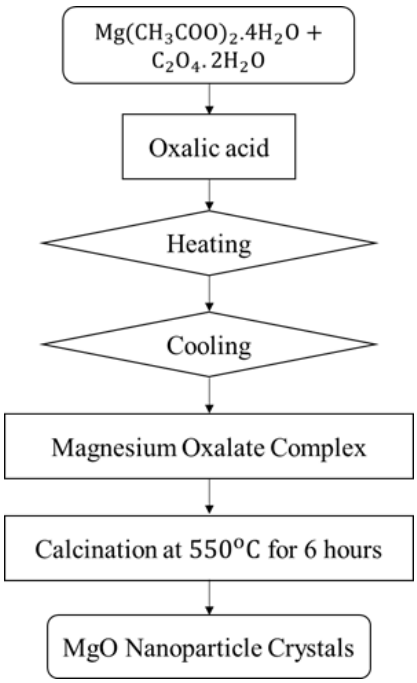

Figure 1. Schematic diagram of the nano-MgO preparation process using the sol-gel method

The solid obtained was heated at 110°C for 24 hours to remove water and acetate trapped in the solid formed, then cooled to room temperature. Furthermore, the dry product was crushed slowly using a mortar and pestle to produce fine powder and then sieved ± 100 mesh to produce a magnesium oxalate complex which functions as a precursor for the manufacture of MgO nanoparticles. The complex formed is then calcined at certain temperatures: 400; 450; 500; 550°C, but in the experiments conducted by

Sutapa et al. (2018), the calcination temperature can be carried out at 550°C with a pressure of 1 atm for 6 hours [31]. This process will produce MgO nanoparticle crystals. Schematically, the production of MgO nanoparticles by the sol-gel method is shown in Figure 1.

2.2. Mathematical Models for Designing Heat Exchangers

In this study, the hot fluid used is propylene glycol and the cold fluid is water. Hot fluid enters at 110°C and leaves at 300°C. Cold fluid enters at 125°C and leaves at 90°C. Table 1 shows the assumptions used for the characteristics of fluids operating in HE. The incoming propylene glycol flow rate was 33.43 (kg/s) while the incoming water flow rate was 7.0 (kg/s). For the process of collecting data regarding specifications, this study refers to the Standard Tubular Exchanger Manufacturers Association (TEMA), while for thermal analysis manual calculations are carried out using Microsoft Excel software. The calculated heat exchange parameters can be seen in Table 2.

Table 1. Assumptions of fluid characteristics working on heat exchanger

	Shell side	Tube side
	Hot fluid	**Cold fluid**
Inlet Temperature, T_{in} (K)	383	398
Outlet Temperature, T_{out} (K)	573	363
Fluid Flow Rate (kg/s)	33,43	7,0
Operating Pressure (atm)	1	1
Specific Heat (kJ/kg.K)	2180	4181
Density (kg/m^3)	1.117	937,2

Table 2. Calculation of heat exchanger parameters

Section	Parameters	Equation	Eq.
Basic Parameters	The energy transferred (Q)	$Q_{in} = Q_{out}$ $m_c \; x \; C_{pc} \; x \; \Delta T_c = m_h \; x \; C_{ph} \; x \; \Delta T_h$ where, Q = the energy transferred (Wt) m = the mass flow rate of the fluid (Kg/s) Cp = the specific heat ΔT = the fluid temperature difference (°C)	(1)
	Logarithmic mean temperature differenced (LMTD)	$LMTD = \frac{(T_{hi} - T_{ci}) - (T_{ho} - T_{co})}{ln \frac{(T_{hi} - T_{ci})}{(T_{ho} - T_{co})}}$ Dimana, T_{hi} = temperature of the hot fluid inlet (°C) T_{ho} = temperature of the hot fluid outlet (°C) T_{ci} = temperature of the cold fluid inlet (°C) T_{co} = temperature of the cold outlet (°C)	(2)

	Correction factor	$R = \frac{T_{hi} - T_{ho}}{T_{ci} - T_{co}}$ $P = \frac{T_{hi} - T_{ho}}{T_{ci} - T_{co}}$ $F = \frac{\sqrt{R^2+1}\ln\left[\frac{1-P}{1-PR}\right]}{(R-1)\ln\left(\frac{2-P\ (R+1-\sqrt{R^2+1})}{2-P(R+1+\sqrt{R^2+1})}\right)}$	(3) (4) (5)
	Heat Transfer Field Area (A)	$A = \frac{Q}{U\ x\ LTMD}$ where, Q = the energy transferred (W) U = the overall heat transfer coefficient LMTD = the logarithmic mean temperature Difference	(6)
	Number of Tubes (N)	$N = \frac{A}{\pi\ x\ D_0 x\ l}$ where, N = the number of tubes A = the area of the heat transfer (m^2) π = 3.14 D_0 = tube diameter (m) l = tube diameter (m)	(7)
	Diameter shell	$D_s = 0{,}63\left(\frac{\sqrt{\frac{CL}{CTP}\ x\ ((A\ x\ PR^2\ xD_o}}{l}\right)^{1/2}$ where, D_s = shell diameter (m) A = the area of the heat transfer area (m^2) P, R = the correction factor Do = tube diameter (m) CTP = one tube (0,93); two tube (0,90); and three tube (0,85) CL = 90° and 45° = 1,00; 30° and 60° = 0,87	(8)
Tube	Total Heat Transfer Surface Area in Tube (A_t)	$a_t = N_t \frac{a'_n}{n}$ where, a_t = = the total heat transfer surface area in the tube (m^2) Nt = the number of tubes a'_n = the flow area in the tube (m^2) n = the number of passes	(9)
	Mass Flow Rate of Water in Tube (Gt)	$G_t = \frac{m_h}{a_t}$ where,	(10)

		G_t = the mass flow of water in the tube (kg/m^{2}s) m_h = the mass flow rate of the hot fluid ((Kg/s) a_t = the flow area tube (m^2)	
	Reynold number (Re, t)	$$Re_t = \frac{di_t \; x \; G_t}{\mu}$$ where, Re_t = = the Reynolds number in tube di_t = the inner tube diameter (m) G_t = the mass flow of water in the tube (m^2) μ = the dynamic viscosity (Kg/ms)	(11)
	Prandtl Number (Pr, t)	$$Pr = \left(\frac{Cp \; x \; \mu}{K}\right)^{1/2}$$ where, Pr = Prandtl number Cp = the specific heat of the fluid in the tube μ = = the dynamic viscosity of the fluid in the tube (Kg/ms) K = the thermal conductivity of the tube material (W/m°C)	(12)
	Nusselt number (Nu, t)	$$Nu = \; 0{,}023 \; x \; {Re_t}^{0,6} \; x \; Pr^{0,33}$$	(13)
	Convection Heat Transfer Coefficient in Tube *(h_i)*	$$hi = \frac{Nu \; x \; K}{d_i, t}$$ where, hi = the convection heat transfer coefficient in the tube (W/m^2°C) K = the thermal conductivity of the material (W/m°C) d_i, t = the inner tube diameter (m)	(14)
Shell	Shell flow area (A_s)	$$A_s = \frac{d_s \; x \; C \; x \; B}{P_t}$$ where, d_s = shell diameter (m) C = clearance (P_t-d_o) B = a shell bundel Pt = tube pitch (1,25 x d_o) (m).	(15)
	Mass Flow Rate of Water in Shell (Gs)	$$G_s = \frac{m_c}{a_s}$$ where, m_c = the mass flow rate of the cold fluid (Kg/s) A_s = the shell flow area (m^2)	(16)

	Equivalent diameter (d_e)	$d_e = \frac{4\left(\frac{Pt}{2}\ x\ 0{,}87\ Pt\ x\ \frac{1}{2}\pi\frac{d_{o.t}}{4}\right)}{\frac{1}{2}\pi d_{o.t}}$ where, Pt = tube pitch (1,25 x d_o) (m) $\pi = 3{,}14$ $d_{o.t}$ = tube outside diameter (m)	(17)
	Reynolds number in shell (Re, s)	$Re_s = \frac{di_s\ x\ G_s}{\mu}$ where, Re_s = Reynolds number in shell di_s = inner tube diameter (m) G_s = mass flow of water in the shell (kg/m^{2}s) μ = dynamic viscosity (kg/ms)	(18)
	Prandtl numbers in shell (Pr, s)	$Pr_s = \left(\frac{Cp\ x\ \mu}{K}\right)^{1/2}$ where, Pr_s = Prandtl number Cp = specific heat of fluid μ = dynamic viscosity of the liquid (Kg/ms) K = thermal conductivity (W/m°C)	(19)
	Nusselt number in the shell (Nu, s)	$Nu = 0{,}023\ x\ {Re_s}^{0,6}\ x\ Pr^{0,33}$ Re_s = Reynold number Pr = Prandtl number	(20)
	Convection Heat Transfer Coefficient in the shell (h_o)	$ho = \frac{Nu\ x\ K}{d_e}$ where, ho = heat transfer coefficient (W/m^2°C) K = thermal conductivity of the material (W/m°C) d_e = diameter equivalent (m)	(21)
Shell and Tube	Actual Overall Heat Transfer Coefficient (U_{act})	$U_{act} = \frac{1}{\frac{1}{h_i} + \frac{\Delta r}{k} + \frac{1}{h_o}}$ where, h_i = inside heat transfer coefficient (W/m^2°C) h_o = outside heat transfer coefficient (W/m^2°C), Δr = wall thickness (m) K = thermal conductivity (W/m°C)	(22)
Heat rate	Hot Fluid rate (C_h)	$C_h = m_h\ .\ Cp_h$ where, C_h = hot fluid rate (W/°C) Cp_h = specific heat capacity (J/Kg°C) m_h = mass flow rate of hot fluid (Kg/s)	(23)

	Cold Fluid Rate (C_C)	$C_c = m_c \,.\, Cp_c$ where, C_c = cold fluid rate (W/°C) m_c = mass flow rate of cold fluid ((J/Kg°C) Cp_c = specific heat capacity (Kg/s).	(24)
		$Q_{max} = C_{min}(Th_i - Tc_i)$ where, Q_{max}= maximum heat transfer (W) C_{min} = minimum heat capacity rate (W/°C) Th_i = temperature of the hot fluid inlet (°C) Tc_i = temperature of the cold fluid inlet (°C).	(25)
Heat Exchanger	Effectivines (ε)	$\varepsilon = \frac{Q_{act}}{Q_{max}} x\ 100\%$ where, Q_{act} = actual energy transferred (W) Q_{max} = maximum heat transfer (W)	(26)
	Number Transfer Unit (NTU)	$NTU = \frac{U\ x\ A}{C_{min}}$ where, U = overall heat transfer coefficient (W/m^2°C) A = heat transfer area (m^2) C_{min} = minimum heat capacity rate (W/°C).	(27)

3. Results and discussion

Calculations show the value of the energy transferred (Q) of 29267 W with a shell length of 0.228 mm; shell diameter 0.203 mm; outer tube diameter 0.0254 m; and the diameter of the inner tube is 0.0211 mm. The wall thickness, tube length and tube pitch used were 0.0021 mm each; 5.4864 m; and 0.02778. This research resulted in an HE effectiveness value of 93.70% which shows the actual heat transfer rate divided by the maximum heat transfer rate. The total HE performance is also determined by the thermal conductivity, viscosity, density, and specific heat of the fluid. The complete calculation results are shown in Table 3.

The HE design model that can be designed is shown in Figure 2. Synthesis of MgO requires a heating temperature of 110ºC and then cooling to 125ºC. In the synthesis of MgO, the hot fluid used is propylene glycol and the cold fluid is water. Hot fluid enters at 110ºC and leaves at 300ºC. Meanwhile, cold fluid enters at 125ºC and leaves at 90ºC. After forming the magnesium oxalate complex, it was continued with calcination at 550ºC for 6 hours. Therefore, the HE with shell and tube one pass meets the requirements and standards based on effectiveness, however the fouling factor has not been calculated.

Table 3. Heat exchanger performance parameters designed based on calculations

No	Parameter	Results
1.	Initial Heat Transfer Rate *(Q)*	29267 W
2.	Logarithmic Mean Temperature Difference *(LMTD)*	12,7 °C
3.	Assumed Overall Fluid Heat Coefficient of Water *(U_a)*	140 Btu/h.ft^2.F
4.	Heat Transfer Field Area *(A)*	132,50 m^2
5.	Number of Tube *(N_t)*	193
6.	Total Heat Transfer Surface Area in Tube *(A_t)*	0,44 m^2
7.	Mass Flow Rate of Water Fluid in Tube *(Gt)*	543,093 kg/m^2.s
8.	Reynold Number in Tube *(Re, t)*	3054,35
9.	Prandtl Number in Tube *(Pr, t)*	6,2670
10.	Nusselt Number in Tube *(Nu, t)*	34,5241
11.	Convection Heat Transfer Coefficient in the Tube *(h_i)*	6590,051 W/m^2°C
12.	Bundle Shell *(Db)*	400,974 mm
13.	Total Heat Transfer Surface Area in Shell *(A_s)*	0,44 m^2
14.	Mass Flow Rate of Water Fluid in Shell *(Gs)*	21,45 kg/m^2.s
15.	Diameter equivalent *(D_e)*	25835,15 m
16.	Reynold Number in Shell *(Re, s)*	553804,45
17.	Prandtl Number in Shell *(Pr, s)*	977,87
18.	Nusselt Number in Shell *(Nu, s)*	709761,26
19.	Convection Heat Transfer Coefficient in Shell *(h_o)*	709761,26 W/m^2°C
20.	Overall Heat Transfer Coefficient Actua *(U_{act})*	7,82
21.	HE Effectiveness (ε)	93,70%
22.	Number of Transfer Unit *(NTU)*	1,308

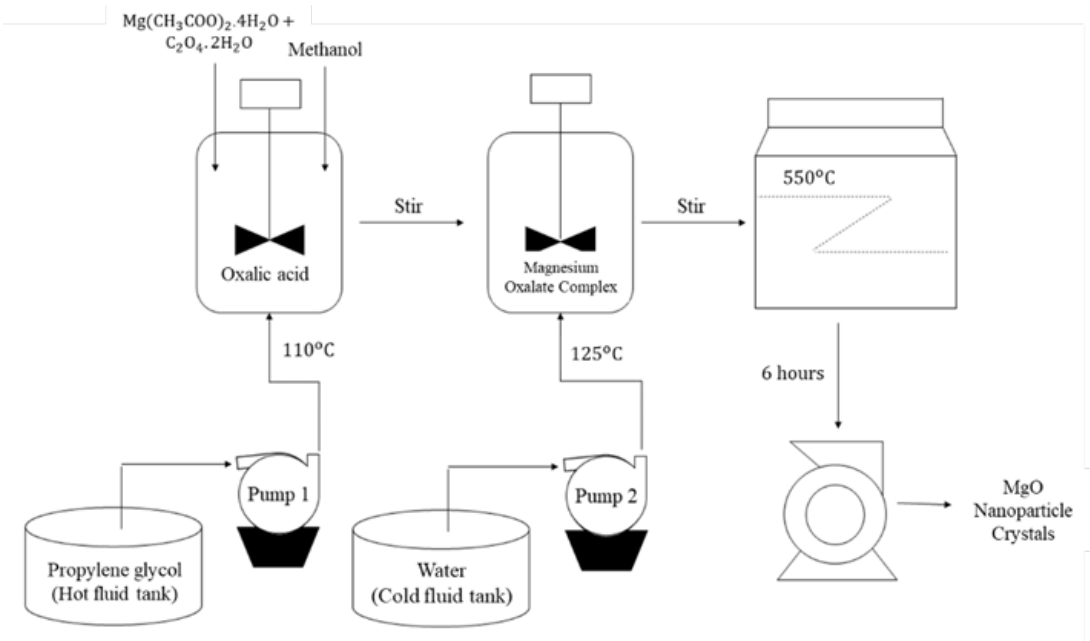

Figure 2. PFD on the synthesis of MgO nanoparticles

4. Conclusion

Calculation of the HE specifications obtained a shell length of 0.228 mm; shell diameter 0.203 mm; outer tube diameter 0.0254 m; inner tube diameter 0.0211 mm; wall thickness 0.0021 mm; tube length 5.4864; and tube pitch 0.02778. Calculations are performed using the Microsoft Excel application. The results show that the HE design on the right shell and tube is of the laminar flow type, with an effectiveness of 93.70%. Thus, the HE with shell and tube one pass meets the standard requirements. This can be seen from several operational parameters according to TEMA standards, namely based on fluid temperature, flow rate, flow regulation, heat exchanger material, tube length, shell and tube diameter, tube number, baffle, and shown to have high effectiveness close to 100%. However, when viewed from a factor perspective, the fouling value has not been calculated. The results of this study are expected to be used as learning media for the design process, operating mechanisms, and HE performance analysis.

References

[1] A. B. D. Nandiyanto, S. R. Putri, R. Ragadhita & T. Kurniawan, Design of heat exchanger for the production of carbon particles. *Journal of Engineering Science and Technology,* 17(4): 2788-2798 (2022).

[2] M. Araiz, Á. Casi, L. Catalán, Á. Martínez, & D. Astrain, Prospects of waste-heat recovery from a real industry using thermoelectric generators: Economic and power output analysis. *Energy Conversion and Management,* 205: 112376 (2020).

[3] Chen, J., Hai, Z., Lu, X., Wang, C., & Ji, X, Heat-transfer enhancement for corn straw slurry from biogas plants by twisted hexagonal tubes. *Applied Energy*, 262, 114554 (2020).

[4] Costa, A. L. H., Tavares, V. B. G., Borges, J. L., Queiroz, E. M., Pessoa, F. L. P., Liporace, F. D. S., & de Oliveira, S. G, Parameter estimation of fouling models in crude preheat trains. *Heat Transfer Engineering*, 34(8-9), 683-691 (2013).

[5] Oh, C. H., Kim, E. S., & Patterson, M, Design option of heat exchanger for the next generation nuclear plant. *Journal of Engineering for Gas Turbines and Power*, 132(3) (2010).

[6] Nandiyanto, A. B. D., Putri, S. R., Ragadhita, R., Maryanti, R., & Kurniawan, T, Design of heat exchanger for the production of synthesis silica. *Journal of Engineering Research* (2021).

[7] Panchal, H., Taamneh, Y., Sathyamurthy, R., Kabeel, A. E., El-Agouz, S. A., Naveen Kumar, P., ... & Bharathwaaj, R, Economic and exergy investigation of triangular pyramid solar still integrated to inclined solar still with baffles. *International Journal of Ambient Energy*, 40(6), 571-576 (2019).

[8] Chin, H. H., Wang, B., Varbanov, P. S., Klemeš, J. J., Zeng, M., & Wang, Q. W, Long-term investment and maintenance planning for heat exchanger network retrofit. *Applied Energy*, 279,

115713 (2020).

[9] Selbaş, R., Kızılkan, Ö., & Reppich, M, A new design approach for shell-and-tube heat exchangers using genetic algorithms from economic point of view. *Chemical Engineering and Processing: Process Intensification*, 45(4), 268-275 (2006).

[10] Alvionita, N., & Astuti, A, Sintesis Nanopartikel Magnesium Oksida (MgO) dengan Metode Presipitasi. *Jurnal Fisika Unand*, 6(1), 89-92 (2017).

[11] Yuan, G., Zheng, J., Lin, C., Chang, X., & Jiang, H, Electrosynthesis and catalytic properties of magnesium oxide nanocrystals with porous structures. *Materials Chemistry and Physics*, 130(1-2), 387-391 (2011).

[12] Zhang, K., An, Y., Zhang, L., & Dong, Q, Preparation of controlled nano-MgO and investigation of its bactericidal properties. *Chemosphere*, 89(11), 1414-1418 (2012).

[13] Mantilaka, M. P. G., De Silva, R. T., Ratnayake, S. P., Amaratunga, G., & de Silva, K. N, Photocatalytic activity of electrospun MgO nanofibres: Synthesis, characterization and applications. *Materials Research Bulletin*, 99, 204-210 (2018).

[14] Mahmoud, H. R., Ibrahim, S. M., & El-Molla, S. A, Textile dye removal from aqueous solutions using cheap MgO nanomaterials: adsorption kinetics, isotherm studies and thermodynamics. *Advanced Powder Technology*, 27(1), 223-231 (2016).

[15] Stankic, S., Müller, M., Diwald, O., Sterrer, M., Knözinger, E., & Bernardi, J, Size-dependent optical properties of MgO nanocubes. *Angewandte Chemie International Edition*, 44(31), 4917-4920 (2005).

[16] Umar, A., Rahman, M. M., & Hahn, Y. B, MgO polyhedral nanocages and nanocrystals based glucose biosensor. *Electrochemistry Communications*, 11(7), 1353-1357 (2009).

[17] Dobrucka, R, Synthesis of MgO nanoparticles using Artemisia abrotanum herba extract and their antioxidant and photocatalytic properties. *Iranian Journal of Science and Technology, Transactions A: Science*, 42(2), 547-555 (2018).

[18] Prasanth, R., Kumar, S. D., Jayalakshmi, A., Singaravelu, G., Govindaraju, K., & Kumar, V. G, Green synthesis of magnesium oxide nanoparticles and their antibacterial activity. (2019).

[19] Balakrishnan, G., Velavan, R., Batoo, K. M., & Raslan, E. H, Microstructure, optical and photocatalytic properties of MgO nanoparticles. *Results in Physics*, 16, 103013 (2020).

[20] Essien, E. R., Atasie, V. N., Okeafor, A. O., & Nwude, D. O, Biogenic synthesis of magnesium oxide nanoparticles using Manihot esculenta (Crantz) leaf extract. *International Nano Letters*, 10(1), 43-48 (2020).

[21] Yunita, F. E., Natasha, N. C., Sulistiyono, E., Rhamdani, A. R., Hadinata, A., & Yustanti, E, Time

and amplitude effect on nano magnesium oxide synthesis from bittern using sonochemical process. *In IOP Conference Series: Materials Science and Engineering*, 858(1), 012045 (2020).

[22] Zhang, H., Hu, J., Xie, J., Wang, S., & Cao, Y, A solid-state chemical method for synthesizing MgO nanoparticles with superior adsorption properties. *RSC Advances*, 9(4), 2011-2017 (2019).

[23] Taghavi Fardood, S., Ramazani, A., & Woo Joo, S, Eco-friendly synthesis of magnesium oxide nanoparticles using arabic Gum. *Journal of Applied Chemical Research*, 12(1), 8-15 (2018).

[24] Mguni, L. L., Mukenga, M., Jalama, K., & Meijboom, R, Effect of calcination temperature and MgO crystallite size on MgO/TiO2 catalyst system for soybean oil transesterification. *Catalysis Communications*, 34, 52-57 (2013).

[25] Caputo, A. C., Pelagagge, P. M., & Salini, P, Heat exchanger design based on economic optimisation. *Applied Thermal Engineering*, 28(10), 1151-1159 (2008).

[26] Jegede, F. O., & Polley, G. T, Optimum heat exchanger design. *Transactions of the Institution of Chemical Engineers*; *(United Kingdom)*, 70(pt A) (1992).

[27] Guo, Z. Y., Liu, X. B., Tao, W. Q., & Shah, R. K, Effectiveness–thermal resistance method for heat exchanger design and analysis. *International Journal of Heat and Mass Transfer*, 53(13-14), 2877-2884 (2010).

[28] Putri, D. B. D. A., & Nandiyanto, A. B, Evaluasi Ekonomi dari Produksi Nanopartikel Magnesium Oksida melalui Metode sol-gel Combustion. *STRING (Satuan Tulisan Riset dan Inovasi Teknologi)*, 4(2), 159-168 (2019).

[29] Febriani, L. I., Nurhashiva, C., Veronica, J., Ragadhita, R., Nandiyanto, A. B. D., & Kurniawan, T, Computation Application: Techno-Economic Analysis on the Production of Magnesium Oxide Nanoparticles by Precipitation Method. *International Journal of Informatics, Information System and Computer Engineering (INJIISCOM)*, 1(1), 117-128 (2020).

[30] Veronica, J., Febriani, L. I., Nurhashiva, C., Ragadhita, R., Nandiyanto, A. B. D., & Kurniawan, T, Practical Computation in the Techno-Economic Analysis of the Production of Magnesium Oxide Nanoparticles using Sol-gel Method. *International Journal of Informatics, Information System and Computer Engineering (INJIISCOM)*, 2(2), 1-12 (2021).

[31] Sutapa, I. W., Wahab, A. W., Taba, P., & La Nafie, N, Synthesis and structural profile analysis of the MgO nanoparticles produced through the sol-gel method followed by annealing process. *Oriental Journal of Chemistry*, 34(2), 1016 (2018).